


Computational screening of two-dimensional coatings for semiconducting photocathodes

Gaoxue Wang , Ping Yang *, and Enrique R. Batista †

Theoretical Division, Los Alamos National Laboratory, Los Alamos, New Mexico 87544, USA

 (Received 28 October 2019; revised manuscript received 20 December 2019; accepted 22 January 2020; published 26 February 2020)

Alkali-based semiconducting photocathodes, due to their high quantum efficiency (QE) in the visible light spectrum, are promising candidates to replace traditional metal photocathodes for high-brightness beam applications such as x-ray free electron lasers (XFELs). However, they suffer from rapid degradation which significantly limits their operational lifetimes. Coating them with two-dimensional (2D) materials has been proposed as a possible avenue to prevent the degradation. Ideally, the 2D coating layer should not increase the work function of semiconducting photocathodes, thus maintaining the high QE of semiconducting photocathodes in visible light. Herein, we report a computational screening of over 4000 2D materials in the Computational 2D Materials Database (C2DB). The assessment of their potential to be good coating layers is based on their effects to the surface electronic properties. We discover several candidate materials that are even capable of decreasing the work function of semiconducting photocathodes. Some of the experimentally synthesized 2D materials, such as hydrogenated graphene (graphane) and several hydroxylated transition metal carbides/nitrides (MXenes), are particularly appealing for this application.

DOI: [10.1103/PhysRevMaterials.4.024001](https://doi.org/10.1103/PhysRevMaterials.4.024001)

I. INTRODUCTION

Photocathodes play a key role in electron accelerators for future light sources, such as x-ray free electron lasers (XFELs) and x-ray energy recovery linacs (XERLs) [1]. Alkali-based semiconducting photocathodes such as cesium antimony (Cs_3Sb) and bialkali antimony (K_2CsSb) have high quantum efficiency (QE) at the level of 1–20% in visible light [2,3], making them prime candidates to replace metallic photocathodes for generating high brightness electron beams [4]. However, these Cs-based semiconducting photocathodes are extremely reactive, particularly with respect to oxygen-containing residual gas molecules even in the ultrahigh vacuum (UHV) conditions inside accelerators, resulting in much shorter operational lifetimes than their metallic counterparts [3,5–9].

Coating with inert two-dimensional (2D) materials is a conceptually attractive approach to improve the lifetimes of semiconducting photocathodes, as schematically shown in Fig. 1(a) [10–12]. In a previous study, we showed how a few layers of hexagonal boron nitride (*h*-BN) can overcome the QE-lifetime tradeoff of alkali-based semiconducting photocathodes [13]. *h*-BN exhibits excellent chemical stability, thus presenting a chemical barrier to prevent the degradation of semiconducting photocathodes from the reactions with residual gases; at the same time, *h*-BN can decrease the work function, thus maintaining the high QE of semiconducting photocathodes in the visible light spectrum. Other popular 2D materials studied, graphene and MoS_2 , increase the work function and shift the photoelectric threshold towards the ultraviolet spectrum, resulting in significant reduction of the

QE in the visible spectrum. This difference between BN and graphene/ MoS_2 was identified to originate from their band alignment with the photocathodes: the conduction band minimum (CBM) of MoS_2 or the Fermi level of graphene is lower than the Fermi level of the photocathodes. This leads to the electron transfer from photocathodes to the coating layers, thus the formation of inward pointing interfacial dipoles that present extra energy barriers for the outward going electrons. In contrast, the CBM of *h*-BN is higher than the Fermi level of the photocathodes, which prevents such electron transfer. Therefore, the band alignment between the photocathodes and the coating layer, as shown in shown in Fig. 1(b), is a crucial criterion for selecting 2D coatings for semiconducting photocathodes [13].

Whereas the experimental approach for finding a suitable coating material is time consuming and less efficient than direct calculation of the physical properties of materials, computational high-throughput screening is getting increasingly popular in materials science thanks to the availability of large material datasets. For this paper, we screened the Computational 2D Materials Database (C2DB) [14] for suitable 2D coating materials for alkali-based semiconducting photocathodes. Several candidate materials besides *h*-BN have been discovered. Especially hydrogenated graphene (graphane), hydrogenated silicon-carbon, hydrogenated germanium-carbon, and several hydroxylated transition metal carbides/nitrides (MXenes) were identified to be promising for this application. The results are important for the development of robust photocathodes for future applications.

II. METHODS

A. Electronic structure calculations

Our calculations were performed with the use of density functional theory (DFT) and projector augmented-wave

*Corresponding author: pyang@lanl.gov

†Corresponding author: erb@lanl.gov

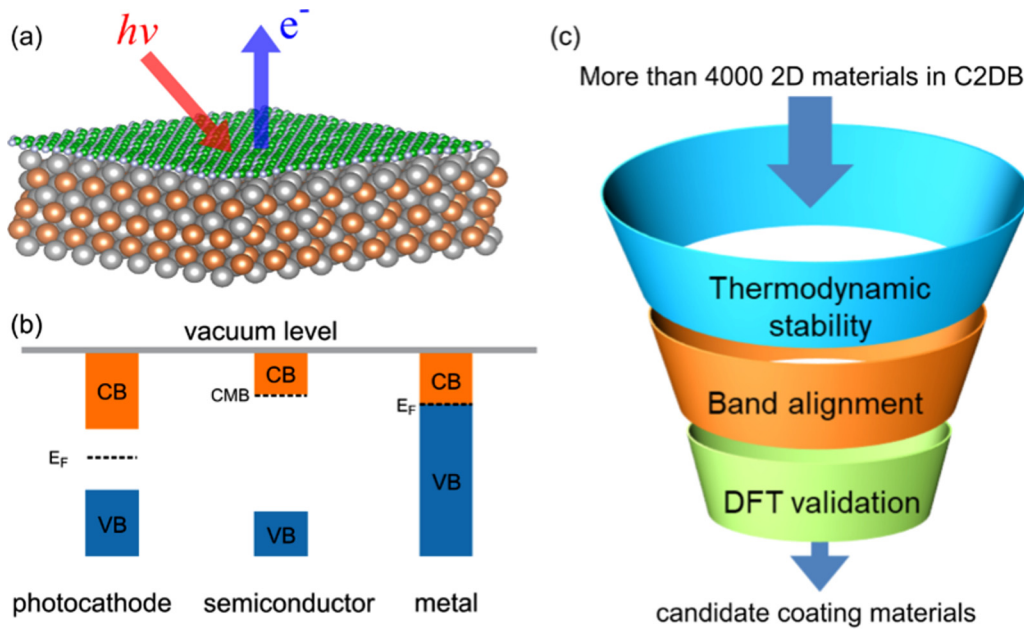


FIG. 1. (a) Schematic illustration of passivating photocathodes with a 2D coating layer, (b) band alignment of semiconducting photocathodes and an ideal semiconducting or metallic coating material, and (c) the computational screening strategy in the C2DB. CB (VB) represents the conduction band (valence band), and E_F is the Fermi level.

(PAW) method [15] as implemented in the Vienna *ab initio* Simulation Package (VASP) [16]. The generalized gradient approximation (GGA) of the Perdew-Burke-Ernzerhof (PBE) [17] functional was used to represent the exchange-correlation interaction. Since the PBE functional could not capture the van der Waals (vdW) interaction [18,19], the DFT-D3 method of Grimme [20] was included in the calculations. Plane-wave basis sets with a cutoff energy of 500 eV were employed [15]. The energy convergence was set to 10^{-6} eV and the residual force on each atom was smaller than 0.01 eV/Å for structural relaxations. The surfaces of photocathodes were represented with slab models with a vacuum gap in the direction normal to the surface. In the supercell, the vacuum distance normal to the slab was larger than 30 Å to eliminate the interactions between the replicas due to the periodic boundary conditions. The Brillouin zone of the supercell was sampled by a uniform Monkhorst-Pack k -point grid [21]. The dipole correction was included to nullify the artificial field imposed on the slab by the periodic boundary conditions [22]. The surfaces were terminated with alkali atoms, which were the most stable surface configurations according to our previous work [9]. The change of work function was also checked with DFT calculations using the HSE06 hybrid functional [23].

B. Screening strategy for 2D coatings

The overall screening strategy is illustrated in Fig. 1(c). The first screening of 2D materials in the C2DB was based on two criteria [13]: (i) band alignment and (ii) thermodynamic and dynamic stability. As mentioned in the previous section, the band alignment between the photocathode and the coating layer plays a critical role. The lowest empty electronic state of the coating layer should be higher than the Fermi level of the photocathode [Fig. 1(b)]. The computed work function of alkali-antimonide photocathodes is in the range of 2–3 eV

depending on the facets [13], which is in agreement with experiments [24]. Therefore, we have employed the criterion of $\text{CBM} > -2.0$ eV for screening semiconducting 2D materials, and Fermi level > -2.0 eV for metallic 2D materials. Note that the energy levels are relative to the vacuum level, which is set to 0 eV. For the second criteria, there are more than 4000 2D materials in the C2DB; some of the materials may be less stable and difficult to be synthesized in the free-standing forms. We therefore have followed the stability criteria in the work by Hastrup *et al.* [14], and only considered materials that are labeled to have a high/medium thermodynamic and dynamic stability (heat of formation < 0.2 eV/atom, minimum eigenvalue of the dynamical matrix > -2.0 eV/Å², and diagonal elements of the elastic constants $C_{ii} > 0$ GPa). Note that the procedure to determine the stability in C2DB provides a necessary but not sufficient condition for the dynamic stability of 2D materials. A rigorous test for the stability requires the calculation of full phonon band structure and elastic stiffness C_{ij} [25]. 2D materials that can pass these two screening criteria are further validated using DFT calculations to ensure that they can provide protection, while not significantly increasing the work function of semiconducting photocathodes.

III. RESULTS AND DISCUSSION

A. Identified 2D coatings

From the over 4000 materials in C2DB, 28 semiconducting 2D materials were identified to have a CBM higher than -2.0 eV at HSE06 level of theory. Their energy levels are shown in Fig. 2. Interestingly, the CBM calculated with the PBE functional is in good agreement to the predictions of the HSE06 functional, whereas the VBM from PBE functional is significantly higher than the results from the HSE06 functional, opening the band gap as expected for the hybrid DFT functional [26]. Among these materials, ten of them have a

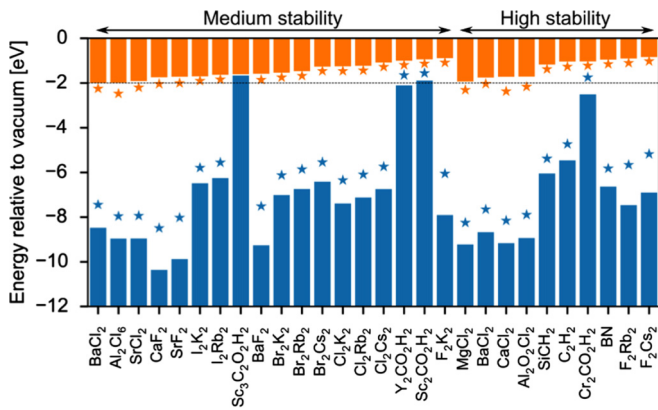


FIG. 2. Energy levels of semiconducting photocathodes screened from the C2DB. The stars are the energy levels calculated from the PBE functional and bars are from the hybrid functional HSE06.

high thermodynamic and dynamic stability (heat of formation < convex hull + 0.2 eV/atom, minimum eigenvalue of the dynamical matrix > -0.01 meV/Å², and $C_{ii} > 0$ GPa), including *h*-BN, chloride monolayers (MgCl₂, BaCl₂, CaCl₂, Al₂O₂Cl₂), hydrogenated monolayers (graphane, SiCH₂), one MXene (Cr₂CO₂H₂), and two alkali fluoride monolayers (Cs₂F₂, Rb₂F₂). The rest of the 2D materials have a medium thermodynamic or dynamic stability. For metallic 2D materials, we identified 21 candidates with Fermi level higher than -2.0 eV. Their energy levels are shown in Fig. 3. All the identified metallic 2D materials are hydroxylated MXenes. Among these, five have a high thermodynamic and dynamic stability, including Mn₂NO₂H₂, V₂CO₂H₂, V₂NO₂H₂, Ti₂CO₂H₂, and Ti₄C₃O₂H₂. The atomic configurations for these identified materials are provided in the Supplemental Material [27].

B. DFT validation

To further evaluate the identified 2D materials as potential coatings, we calculated the change of work function of Cs₃Sb upon coating with 2D materials. Cs₃Sb is a well characterized semiconducting photocathode [9]. We have selected some of the representative 2D materials with a high thermodynamic

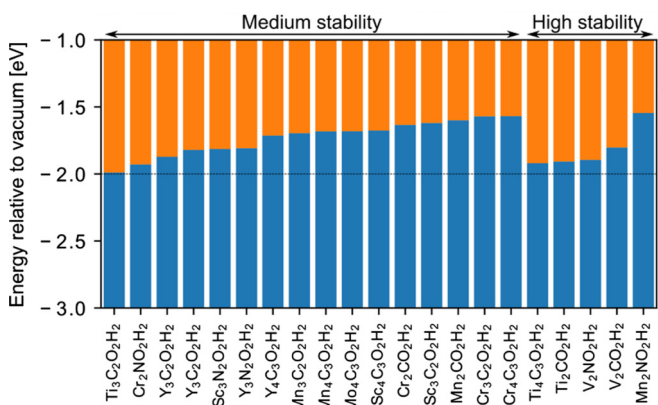


FIG. 3. Energy levels of metallic photocathodes screened from the C2DB.

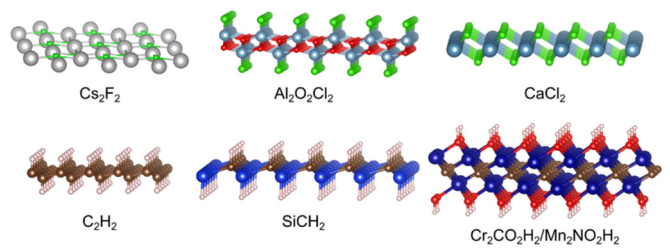


FIG. 4. Representative 2D coating materials for semiconducting photocathodes.

and dynamic stability in Figs. 2 and 3, including semiconducting C₂H₂, SiCH₂, Al₂O₂Cl₂, CaCl₂, Cr₂CO₂H₂, Cs₂F₂, and metallic Mn₂NO₂H₂. Their atomic structures are shown in Fig. 4.

Large supercells that minimize the lattice mismatch between Cs₃Sb surfaces and the coating layers were used to calculate the properties of the coated surfaces, and all the atomic positions in the supercells were fully relaxed. The structures of the uncoated Cs₃Sb (111) surface and the surface after coating with SiCH₂ and Mn₂NO₂H₂ are plotted in Fig. 5. The remaining relaxed structures are shown in Fig. S1 in the Supplemental Material [27]. The work function is calculated as $W = E_{vac} - E_F$, where E_{vac} is the planar averaged electrostatic potential in the vacuum region, and E_F is the Fermi energy as illustrated in Figs. 6(a) and 6(c). The calculated work functions of uncoated Cs₃Sb (111) and (100) surfaces are 2.05 eV and 2.01 eV, respectively, which are in good agreement with the experimental results of 2.1 eV [24].

The change of work function ($\Delta W = W_{coated} - W_{uncoated}$) of Cs₃Sb surfaces upon coating with these 2D materials is summarized in Table I. Several materials were found to decrease the work function, which can lower the barrier for electrons to leave the surface, in effect enhancing the QE. Notably, SiCH₂ [Si-closer configuration, Figs. 6(a) and 6(b)] decreases the work function as much as -0.98 eV at GGA-PBE level of theory, which is even larger than what we

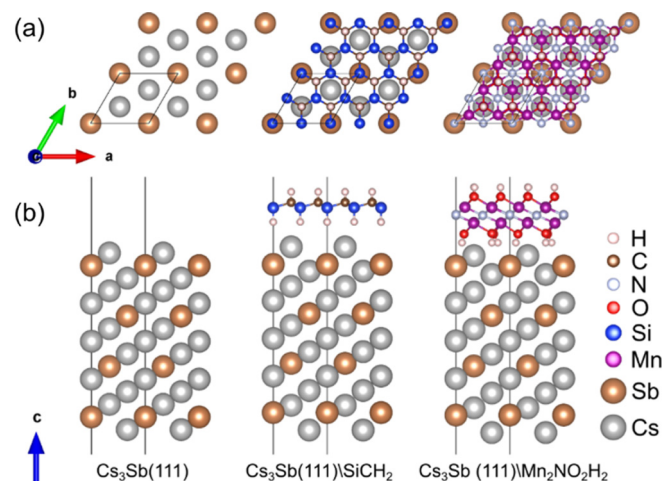


FIG. 5. Top views (a) and side views (b) of uncoated Cs₃Sb (111) surface and SiCH₂ (Si-closer configuration), Mn₂NO₂H₂ coated Cs₃Sb (111) surfaces, respectively.

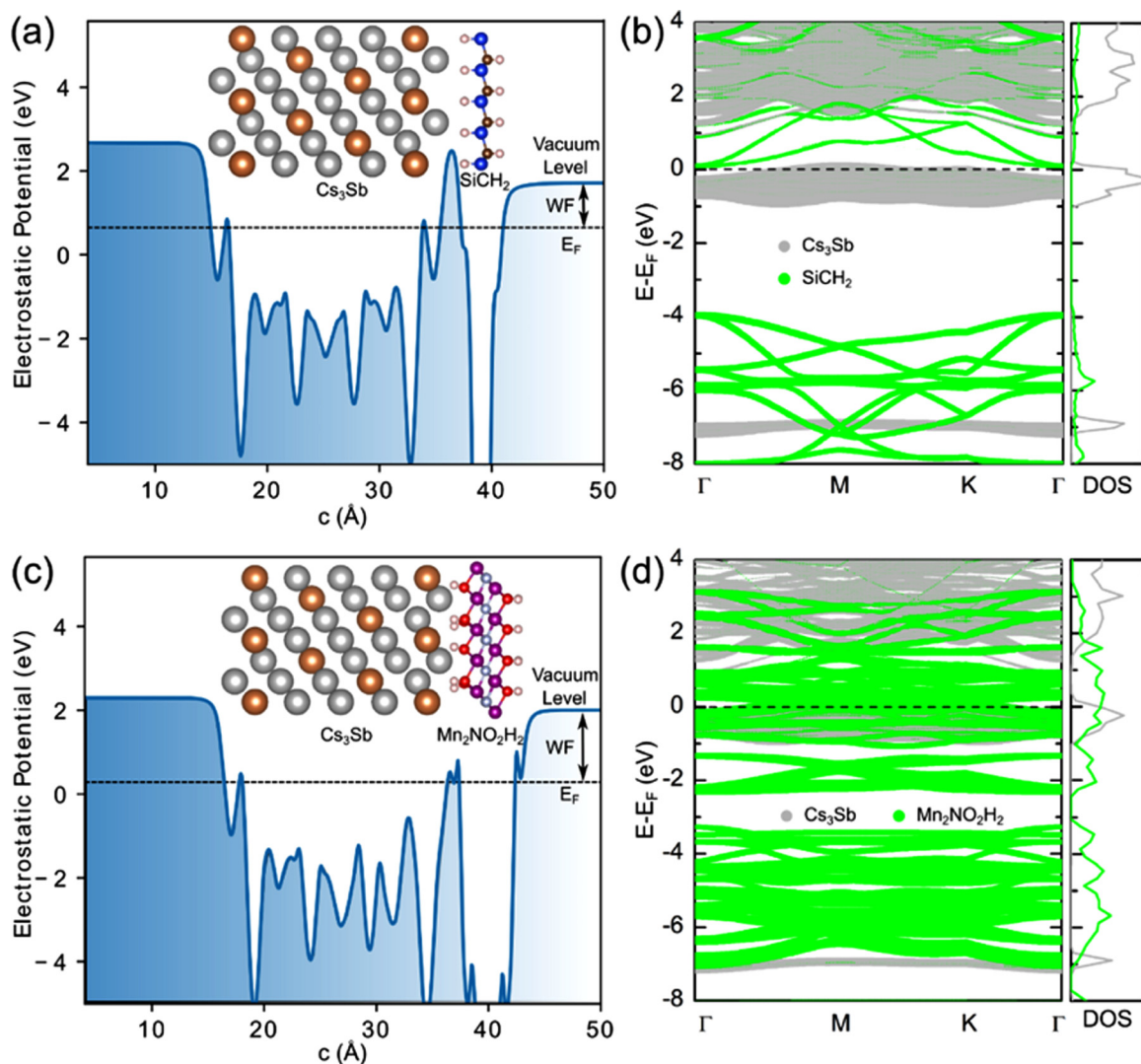


FIG. 6. Planar averaged electrostatic potentials (a,c) and electronic band structures (b,d) of SiCH_2 and $\text{Mn}_2\text{NO}_2\text{H}_2$ coated Cs_3Sb (111) surface.

had previously found for h -BN (-0.4 eV). This is attributed to the buckled structure of SiCH_2 , as seen in Figs. 4 and 5, leading to an intrinsic dipole moment pointing from the Si side to the C side. As seen from the band structure in Fig. 6(b), the Fermi level of the Cs_3Sb - SiCH_2 hybrid structure is below the CBM of SiCH_2 indicating there is no electron transfer from Cs_3Sb to SiCH_2 . In contrast to the Si-closer configuration, coating with the C-closer configuration increases the work function by 1.8 eV. We have also considered the isoelectronic GeCH_2 (Ge-closer configuration) with a structure identical to SiCH_2 . It has a similar effect of decreasing the work function by -0.96 eV.

Compared to graphene, which increases the work function by 1.5 eV, the hydrogenated version (graphane or C_2H_2), is much less intrusive in the electronic properties of the surface, slightly increasing the work function by 0.12 eV using the GGA-PBE functional. The binding energy of the coating layer on photocathodes is defined as $E_b = E_{\text{surface+coating}} - (E_{\text{surface}} + E_{\text{coating}})$, where $E_{\text{surface+coating}}$, E_{surface} , and E_{coating} are the total energies of the complex, the uncoated surface, and the coating layer, respectively. For the hydrogenated

monolayers including C_2H_2 and SiCH_2 , the binding energies are in the range -7.0 to -10 $\text{meV}/\text{\AA}^2$, which are close to the interlayer interactions of graphite (-11.8 $\text{meV}/\text{\AA}^2$) [28], indicating that the hydrogenated monolayers can be attached to the surface of photocathodes through weak vdW interaction. It should be noted that graphane has been synthesized by hydrogenation of graphene [29,30]. Our work predicts new applications of graphane as a coating layer for semiconducting photocathodes.

MXenes are a large family of 2D materials [31–33]. Different methods to functionalize MXenes, such as hydroxylation, have been realized by several groups recently [34–39]. Our calculations yielded that semiconducting $\text{Cr}_2\text{CO}_2\text{H}_2$ and metallic $\text{Mn}_2\text{NO}_2\text{H}_2$ [Figs. 6(c) and 6(d)] decrease the work function by -0.48 and -0.29 eV at GGA-PBE level of theory, respectively. The binding energies of $\text{Cr}_2\text{CO}_2\text{H}_2$ and $\text{Mn}_2\text{NO}_2\text{H}_2$ are -48.24 and -34.21 $\text{meV}/\text{\AA}^2$, respectively. The reduction of work function and negative binding energies of $\text{Cr}_2\text{CO}_2\text{H}_2$ and $\text{Mn}_2\text{NO}_2\text{H}_2$ indicate they are good coatings for semiconducting photocathodes. Since other hydroxylated MXenes that are identified in Figs. 2 and 3

TABLE I. Size of the supercell and k-point grid, binding energy E_b , and change of work function ΔW at PBE and HSE06 level of theory for various 2D materials on Cs₃Sb (111) or (100) surface.

	2D material	Supercell size (\AA^2)	k-point grid	$E_b(\text{meV}/\text{\AA}^2)$	ΔW_{PBE} (eV)	ΔW_{HSE06} (eV)
Semiconductor	<i>h</i> -BN	12.55 \times 13.04 12.95 \times 12.95 (100)	3 \times 3 \times 1	-9.02	-0.40 [13]	-0.81
	graphane (C ₂ H ₂)	12.69 \times 12.69 12.95 \times 12.95 (111)	3 \times 3 \times 1	-8.16	+0.12	+0.06
	SiCH ₂ (Si-closer)	6.26 \times 6.26 6.48 \times 6.48 (111)	7 \times 7 \times 1	-8.31	-0.98	-1.21
	SiCH ₂ (C-closer)	6.26 \times 6.26 6.48 \times 6.48 (111)	7 \times 7 \times 1	-7.66	+1.80	+1.83
	GeCH ₂ (Ge-closer)	6.50 \times 6.50 6.48 \times 6.48 (111)	7 \times 7 \times 1	-7.66	-0.96	-1.26
	Cr ₂ CO ₂ H ₂	6.14 \times 6.14 6.48 \times 6.48 (111)	7 \times 7 \times 1	-48.24	-0.48	+0.02
	Al ₂ O ₂ Cl ₂	18.37 \times 6.35 19.42 \times 6.48 (100)	3 \times 7 \times 1	-14.61	+0.44	+0.09
	CaCl ₂	12.41 \times 12.41 12.95 \times 12.95 (111)	3 \times 3 \times 1	-13.56	+1.16	+0.92
	Cs ₂ F ₂	5.77 \times 5.77 6.48 \times 6.48 (100)	7 \times 7 \times 1	-205.36	-0.54	-0.69
	Metal	Graphene	12.35 \times 12.83 12.95 \times 12.95 (100)	3 \times 3 \times 1	-24.3	+1.50 [13]
Mn ₂ NO ₂ H ₂		6.14 \times 6.14 6.48 \times 6.48 (111)	7 \times 7 \times 1	-34.21	-0.29	-0.34

share similar atomic and electronic structures with Cr₂CO₂H₂ or Mn₂NO₂H₂, they are expected to be good coatings as well.

Cs₂F₂ decreases the work function by -0.54 eV and binds strongly on the Cs₃Sb surface with a binding energy of -205.36 meV/ \AA^2 at GGA-PBE level of theory. Since Cs₂F₂, Rb₂F₂, K₂F₂, Cs₂Cl₂, Rb₂Cl₂, K₂Cl₂, Cs₂Br₂, Cs₂I₂, and Cs₂I₂ have similar semiconducting properties and their CBM values are all above the Fermi level of Cs₃Sb (Fig. 2), forming thin alkali-halide films on alkali-based semiconducting photocathodes is expected to provide protection without decreasing the QE. In fact, previous experiments have demonstrated that alkali-halide coatings can be used to activate and increase the stability of semiconducting photocathodes [40,41].

The chloride monolayers, CaCl₂ and AlO₂Cl₂, were found to increase the work function significantly by 1.16 and 0.44 eV, respectively. We noticed that the CaCl₂ structure was severely distorted upon coating on Cs₃Sb, forming strong Cs-Cl and Ca-Sb bonds (Fig. S1 [27]). Therefore, CaCl₂ and AlO₂Cl₂ are unlikely to be good coatings for alkali-based photocathodes.

It is well known that the band gaps of semiconductors are underestimated using the GGA-PBE functional. We have also checked the change of the work function with the HSE06 hybrid functional [23], which is more reliable for predicting the electronic structure of semiconductors [26]. Due to the high computational cost of using HSE06, we limited the use of it to single-point calculations at the PBE optimized geometries. The corresponding ΔW_{HSE06} are shown in Table I. It is seen that the difference in ΔW_{HSE06} and ΔW_{PBE} is smaller than 0.5 eV for all the structures. The selected hydrogenated monolayers including graphane, SiCH₂ (Si-closer), and GeCH₂ (Ge-closer), and hydroxylated MXenes

Cr₂CO₂H₂ and Mn₂NO₂H₂ decrease or only slightly increase the work function at HSE06 level of theory, thus further validating the 2D materials identified through the procedure in this work to be promising coatings for semiconducting photocathodes.

IV. CONCLUSIONS

In summary, we computationally screened out all the 2D materials in the C2DB dataset that can serve as coatings for alkali-based semiconducting photocathodes. Besides *h*-BN, two families of 2D materials are identified: (i) hydrogenated monolayers, graphane (C₂H₂), SiCH₂, and GeCH₂, and (ii) hydroxylated MXenes. Although graphene significantly increases the work function of alkali-based photocathodes, hydrogenated graphene (graphane) only slightly increases the work function. SiCH₂ and GeCH₂ monolayers can decrease the work function by around -1 eV due to their intrinsic dipole moments. Several metallic or semiconducting hydroxylated MXenes can decrease the work function of Cs₃Sb, suggesting that this family of materials has bright future as protective coatings. Some of the identified materials have already been synthesized, such as graphane [29,30] and hydroxylated MXenes [31–39]. Bianco *et al.* have demonstrated that germanane, a germanium graphane analogue [42], only slowly oxidizes in air over the span of 5 months, indicating good degradation resistance of hydrogenated monolayers. Lipatov *et al.* have reported that hydroxylated MXenes have reasonable stability and remain their electronic properties even after exposure to air for more than 24 hours [43]. Considering the reduction of work function and the good degradation resistance, hydrogenated monolayers and hydroxylated MXenes are promising 2D coatings for

semiconducting photocathodes. Our computational screening can guide the design of photocathodes with elongated lifetimes and high QE in the visible light spectrum for accelerator applications.

ACKNOWLEDGMENTS

The authors gratefully acknowledge funding for this project from the Laboratory Directed Research and

Development program of Los Alamos National Laboratory (LANL) under Projects No. 20180007DR and No. 20190079DR. LANL is operated by Triad National Security, LLC, for the National Nuclear Security Administration of US Department of Energy (Contract No. 89233218CNA000001). G.W. thanks the Director's Postdoc Fellow from LANL. The calculations were performed using EMSL (grid.436923.9), a DOE Office of Science User Facility sponsored by the Office of Biological and Environmental Research.

-
- [1] P. Musumeci, J. G. Navarro, J. Rosenzweig, L. Cultrera, I. Bazarov, J. Maxson, S. Karkare, and H. Padmore, *Nucl. Instrum. Methods Phys. Res., Sect. A* **907**, 209 (2018).
- [2] R. Xiang and J. Teichert, *Phys. Procedia* **77**, 58 (2015).
- [3] P. Michelato, *Nucl. Instrum. Methods Phys. Res., Sect. A* **393**, 455 (1997).
- [4] B. E. Carlsten, E. R. Colby, E. H. Esarey, M. Hogan, F. X. Kartner, W. S. Graves, W. P. Leemans, T. Rao, J. B. Rosenzweig, C. B. Schroeder, D. Sutter, and W. E. White, *Nucl. Instrum. Methods Phys. Res., Sect. A* **622**, 657 (2010).
- [5] V. Pavlenko, F. Liu, M. A. Hoffbauer, N. A. Moody, and E. R. Batista, *AIP Adv.* **6**, 115008 (2016).
- [6] L. R. Danielson, C. Lee, and P. E. Oettinger, *Appl. Surf. Sci.* **16**, 257 (1983).
- [7] S. Pastuszka, A. S. Terekhov, and A. Wolf, *Appl. Surf. Sci.* **99**, 361 (1996).
- [8] D. Durek, F. Frommberger, T. Reichelt, and M. Westermann, *Appl. Surf. Sci.* **143**, 319 (1999).
- [9] G. Wang, R. Pandey, N. A. Moody, and E. R. Batista, *J. Phys. Chem. C* **121**, 8399 (2017).
- [10] H. Yamaguchi, F. Liu, J. DeFazio, C. Villarrubia, D. Finkenstadt, K. L. Jensen, V. Pavlenko, M. Mehl, S. Lambrakos, G. Gupta, A. D. Mohite, and N. A. Moody, *npj 2D Mater. Appl.* **1**, 12 (2017).
- [11] F. Liu, N. A. Moody, K. L. Jensen, V. Pavlenko, C. W. Narvaez Villarrubia, A. D. Mohite, and G. Gupta, *Appl. Phys. Lett.* **110**, 041607 (2017).
- [12] H. Yamaguchi, F. Liu, J. DeFazio, M. Gaowei, C. W. N. Villarrubia, J. Xie, J. Sinsheimer, D. Strom, V. Pavlenko, K. L. Jensen, J. Smedley, A. D. Mohite, and N. A. Moody, *Adv. Mater. Interfaces* **5**, 1800249 (2018).
- [13] G. Wang, P. Yang, N. A. Moody, and E. R. Batista, *npj 2D Mater. Appl.* **2**, 17 (2018).
- [14] S. Haastrup, M. Strange, M. Pandey, T. Deilmann, P. S. Schmidt, N. F. Hinsche, M. N. Gjerding, D. Torelli, P. M. Larsen, A. C. Riis-Jensen, J. Gath, K. W. Jacobsen, J. J. Mortensen, T. Olsen, and K. S. Thygesen, *2D Mater.* **5**, 042002 (2018).
- [15] G. Kresse and D. Joubert, *Phys. Rev. B* **59**, 1758 (1999).
- [16] G. Kresse and J. Furthmüller, *Comput. Mater. Sci.* **6**, 15 (1996).
- [17] J. P. Perdew, K. Burke, and M. Ernzerhof, *Phys. Rev. Lett.* **77**, 3865 (1996).
- [18] B. Sachs, T. O. Wehling, M. I. Katsnelson, and A. I. Lichtenstein, *Phys. Rev. B* **84**, 195414 (2011).
- [19] G. Giovannetti, P. A. Khomyakov, G. Brocks, P. J. Kelly, and J. van den Brink, *Phys. Rev. B* **76**, 073103 (2007).
- [20] S. Grimme, *J. Comput. Chem.* **27**, 1787 (2006).
- [21] H. J. Monkhorst and J. D. Pack, *Phys. Rev. B* **13**, 5188 (1976).
- [22] L. Bengtsson, *Phys. Rev. B* **59**, 12301 (1999).
- [23] J. Heyd, G. E. Scuseria, and M. Ernzerhof, *J. Chem. Phys.* **118**, 8207 (2003).
- [24] J. Teichert, R. Xiang, G. Suberlucq, and J. W. Verschuur, CARE Note-2004-033-PHIN, http://esgard.lal.in2p3.fr/Project/Activities/Current/Deliverables/CARE_Deliverables.htm, 2004.
- [25] F. Mouhat and F.-X. Coudert, *Phys. Rev. B* **90**, 224104 (2014).
- [26] J. Heyd, J. E. Peralta, G. E. Scuseria, and R. L. Martin, *J. Chem. Phys.* **123**, 174101 (2005).
- [27] See Supplemental Material at <http://link.aps.org/supplemental/10.1103/PhysRevMaterials.4.024001> for the coordinates of selected 2D materials and some of the relaxed surfaces.
- [28] Z. Liu, J. Z. Liu, Y. Cheng, Z. Li, L. Wang, and Q. Zheng, *Phys. Rev. B* **85**, 205418 (2012).
- [29] D. C. Elias, R. R. Nair, T. M. G. Mohiuddin, S. V. Morozov, P. Blake, M. P. Halsall, A. C. Ferrari, D. W. Boukhvalov, M. I. Katsnelson, A. K. Geim, and K. S. Novoselov, *Science* **323**, 610 (2009).
- [30] M. Pumera and C. H. A. Wong, *Chem. Soc. Rev.* **42**, 5987 (2013).
- [31] J. Halim, S. Kota, M. R. Lukatskaya, M. Naguib, M. Zhao, E. J. Moon, J. Pitock, J. Nanda, S. J. May, Y. Gogotsi, and M. W. Barsoum, *Adv. Funct. Mater.* **26**, 3118 (2016).
- [32] M. Naguib, J. Come, B. Dyatkin, V. Presser, P.-L. Taberna, P. Simon, M. W. Barsoum, and Y. Gogotsi, *Electrochem. Commun.* **16**, 61 (2012).
- [33] B. Anasori, Y. Xie, M. Beidaghi, J. Lu, B. C. Hosler, L. Hultman, P. R. Kent, Y. Gogotsi, and M. W. Barsoum, *ACS Nano* **9**, 9507 (2015).
- [34] J. Zhou, X.-H. Zha, M. Yildizhan, P. Eklund, J. Xue, M. Liao, P. O. Å. Persson, S. Du, and Q. Huang, *ACS Nano* **13**, 1195 (2019).
- [35] Q. Peng, J. Guo, Q. Zhang, J. Xiang, B. Liu, A. Zhou, R. Liu, and Y. Tian, *J. Am. Chem. Soc.* **136**, 4113 (2014).
- [36] X. Jiang, S. Liu, W. Liang, S. Luo, Z. He, Y. Ge, H. Wang, R. Cao, F. Zhang, Q. Wen, J. Li, Q. Bao, D. Fan, and H. Zhang, *Laser Photonics Rev.* **12**, 1700229 (2018).
- [37] T. Li, L. Yao, Q. Liu, J. Gu, R. Luo, J. Li, X. Yan, W. Wang, P. Liu, B. Chen, W. Zhang, W. Abbas, R. Naz, and D. Zhang, *Angew. Chem. Int. Ed.* **57**, 6115 (2018).
- [38] J. L. Hart, K. Hantanasirisakul, A. C. Lang, B. Anasori, D. Pinto, Y. Pivak, T. van Ommen, S. J. May, Y. Gogotsi, and M. L. Taheri, *Nat. Commun.* **10**, 522 (2019).

- [39] T. Habib, X. Zhao, S. A. Shah, Y. Chen, W. Sun, H. An, J. L. Lutkenhaus, M. Radovic, and M. J. Green, [npj 2D Mater. Appl.](#) **3**, 8 (2019).
- [40] T. Kaisheng, *J. Electron.* **5**, 53 (1988).
- [41] E. Shefer, A. Breskin, T. Boutboul, R. Chechik, B. Singh, H. Cohen, and I. Feldman, *J. Appl. Phys.* **92**, 4758 (2002).
- [42] E. Bianco, S. Butler, S. Jiang, O. D. Restrepo, W. Windl, and J. E. Goldberger, *ACS Nano* **7**, 4414 (2013).
- [43] A. Lipatov, M. Alhabeab, M. R. Lukatskaya, A. Boson, Y. Gogotsi, and A. Sinitskii, *Adv. Electron. Mater.* **2**, 1600255 (2016).